Available online at www.sciencedirect.com
ScienceDirect
Applied Surface Science 254 (2008) 4891–4898
applied surface science
www.elsevier.com/locate/apsusc

Optical and AFM study of electrostatically assembled films of CdS and ZnS colloid nanoparticles

Suryajaya [a,*], A. Nabok [a], F. Davis [b], A. Hassan [a], S.P.J. Higson [b], J. Evans-Freeman [a]

[a] *Materials and Engineering Research Institute, Sheffield Hallam University, City Campus, Howard Street, Sheffield S1 1WB, UK*
[b] *Cranfield Health, Cranfield University, Silsoe, Bedfordshire MK45 4DT, UK*

Received 30 November 2007; received in revised form 26 January 2008; accepted 26 January 2008
Available online 5 February 2008

Abstract

CdS and ZnS semiconducting colloid nanoparticles coated with the organic shell, containing either SO_3^- or NH_2^+ groups, were prepared using the aqueous phase synthesis. The multilayer films of CdS (or ZnS) were deposited onto glass, quartz and silicon substrates using the technique of electrostatic self-assembly. The films produced were characterized with UV–vis spectroscopy, spectroscopic ellipsometry and atomic force microscopy. A substantial blue shift of the main absorption band with respect to the bulk materials was found for both CdS and ZnS films. The Efros equation in the effective mass approximation (EMA) theoretical model allowed the evaluation of the nanoparticle radius of 1.8 nm, which corresponds well to the ellipsometry results. AFM shows the formation of larger aggregates of nanoparticles on solid surfaces.

PACS : 73.61.Ga; 78.20.Ci; 78.67.Hc

Keywords: Colloid nanoparticles; Electrostatic self-assembly; Quantum confinement; Ellipsometry

1. Introduction

In the past decade, II–VI semiconductor nanoparticles have attracted much attention because of their size-dependent and thus tuneable photo- and electro-luminescence properties and promising applications in optoelectronics [1,2]. The main absorption and luminescent bands of such materials can be easily controlled by their composition and particle size to enable the fabrication of light emitting diodes (LEDs) of required colour [3] or white light LEDs covering the whole visible spectral range [4]. II–VI semiconductor quantum dots, especially CdS and ZnS, have been synthesized using different methods, such as embedded in polymers [5] or zeolites [6], reverse micelles [7,8] and the method of arrested precipitation in suitable organic moieties [9,10] including alkylthiols, phosphines, phosphine oxides, phosphates, phosphonates, amides or amines, carboxylic acids, and nitrogen-containing aromatics [9–14]. Amongst these methods, the approach of arrested precipitation, that uses thiols as surface passivating ligands, gives the narrowest size distribution with a standard deviation of only about ±5–7% [10]. This method can be divided into two groups, non-aqueous [9,10], and aqueous [10–13]. The size and shape of nanoparticles can be controlled by the composition of surfactant molecules and the time of growth [8,15,16].

Since colloid nanoparticles are dispersed in solution, they can be produced in large quantities, and later transferred to any desired substrate using suitable deposition techniques. Electrostatic self-assembly (ESA) of colloid nanoparticles is particularly attractive method enabling the deposition of pre-synthesized electrically charged colloid nanoparticles of different II–VI semiconducting materials by alternation with oppositely charged layers of polycations (or polyanions) [17–20].

In this work, an aqueous-phase synthesis of colloid nanoparticles was used [12,14]. A small modification of the synthesis procedure allowed the formation of CdS and ZnS colloid nanoparticles coated with the organic shell containing either SO_3^- or NH_2^+ groups and thus suitable for electrostatic self-assembly. This makes possible the deposition of multilayered films of cationic and anionic nanopar-

* Corresponding author. Tel.: +44 114 225 3254.
E-mail addresses: s.suryajaya@shu.ac.uk, suryajaya@gmail.com (Suryajaya).

0169-4332/$ – see front matter © 2008 Elsevier B.V. All rights reserved.
doi:10.1016/j.apsusc.2008.01.134

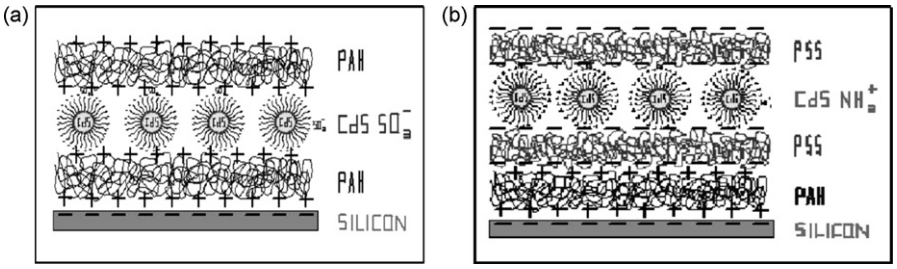

Fig. 1. Deposition of colloid nanoparticles CdS–SO_3^- (a) and CdS–NH_2^+ (b).

ticles alternated with the polyanions and polycations, respectively, as well as the deposition of nanoparticles even without intermediate binding polyelectrolyte layers. Such approach can be useful in future for the formation of semiconductor superlattices.

We present here the systematic study of several combinations of CdS and ZnS nanostructured thin films. For the first time, spectroscopic ellipsometry, along with the UV–vis absorption spectroscopy, were deployed to study optical properties of such nanostructures. Morphology of the obtained films was assessed using tapping mode atomic force microscopy (AFM).

2. Experimental details

2.1. Preparation of colloid nanoparticles

CdS–SO_3^- and ZnS–SO_3^- colloid nanoparticles were prepared by mixing an aqueous solution of 0.02 M sodium 2-mercapto-ethane-sulfonate with 0.04 M solution of either $CdCl_2$ or $ZnCl_2$. A 0.04 M solution of sodium sulphide was then added dropwise to the mixture while it is stirred. Colloid nanoparticles of CdS–NH_2^+ and ZnS–NH_2^+ were made the same way but using 0.02 M cysteamine hydrochloride as a capping agent. All chemicals used were of high purity purchased from Sigma–Aldrich. Solutions were prepared using deionised Millipore water, having resistance of no less than 18 MΩ, at room temperature.

2.2. Deposition method

In this work, the electrostatic self-assembly is used as a deposition technique. Firstly, the substrates (glass and quartz slides, and silicon wafers) were treated in 1% KOH solution in 60% ethanol to enhance their natural negative charge on the surface associated with the OH^- groups [21]. Two types of polyelectrolytes were used as binding layers for electrostatic layer-by-layer deposition of CdS and ZnS nanoparticles [17,18]: polycation poly-allylamine hydrochloride (PAH) and polyanions poly-styrene-sulfonate sodium salt (PSS), both purchased from Sigma–Aldrich. First, a layer of PAH was deposited on the negatively charged substrate by dipping the sample for 20 min into 1 M aqueous solution of PAH, which makes the surface positively charged. Then negatively charged CdS–SO_3^- (or ZnS–SO_3^-) nanoparticles can be deposited straight onto the PAH layer by dipping the substrate into respective colloid solution for 10 min (see Fig. 1). Multilayered films of CdS–SO_3^-/PAH or ZnS–SO_3^-/PAH CdS can be produced by repeating these two deposition steps with intermediate rinsing the sample in Millipore deionised water. The exposure time in all consecutive dipping was 10 min.

In order to deposit positively charged nanoparticles, CdS–NH_2^+ and ZnS–NH_2^+, a positively charged substrate (after deposition of the first PAH layer) should be dipped into 1 M aqueous solution of PSS for 10 min. This alters the polarity of the surface charge, and a layer of either CdS–NH_2^+ or ZnS–NH_2^+ nanoparticles can be directly deposited on such substrate. Multilayered films of CdS–NH_2^+/PSS (or ZnS–NH_2^+/PSS) can be produced by repeating these two steps. After each deposition step, all samples were thoroughly rinsed with Millipore water, having the resistance of no less than 18 MΩ. After completing the deposition, all samples were left to dry in the clean environment at room temperature.

2.3. Experimental methods

UV–vis absorption spectra of the films deposited onto glass and quartz substrates were recorded using Varian CARY 50 spectrophotometer. In the case of ZnS particles, having the main absorption band in the near-UV wavelength range, quartz substrates were used.

Optical parameters of the films obtained were studied with the spectroscopic ellipsometry. The measurements were carried out on films deposited on pieces of silicon wafers using the J.A. Woollam M2000V rotating compensator spectroscopic instrument, which operates in the spectral range of 370–1000 nm. The angle of incidence of 70° was used. The film parameters, such as thickness (d) and the spectra of the refractive index (n) and the extinction coefficient (k)[1] were evaluated from the experimental spectra of two ellipsometric parameters Ψ and Δ representing, respectively, the amplitude (A) ratio and phase (φ) shift between p- and s-components of polarised light:

$$\psi = \arctan\left(\frac{A_p}{A_s}\right), \quad \Delta = \varphi_p - \varphi_s \tag{1}$$

The procedure of fitting of the experimental $\Psi(\lambda)$ and $\Delta(\lambda)$ spectra consists of solving numerically the main ellipsometry

[1] n and k are the components of complex index of refraction $N = n - jk$.

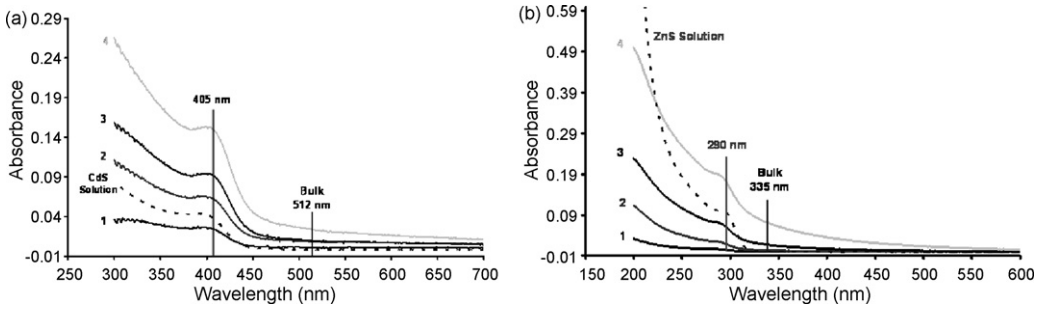

Fig. 2. UV–vis absorption spectra of PAH/CdS–SO_3^- film (a) and PAH/ZnS–SO_3^- film (b). The numbers near respective spectra correspond to the number of polyelectrolyte/nanoparticle bilayrs.

equation

$$\tan(\psi)\exp(i\Delta) - \frac{R_p}{R_s}, \tag{2}$$

in which Fresnel reflection coefficients, R_p and R_s for p- and s-components of polarized light, respectively, are related to the parameters of the reflecting system (d, n, and k) through Fresnel equations [22]. Commercial VWASE32® software provided by J.A. Woollam Co [23] was used for data fitting.

AFM images of the layers deposited on silicon were recorded with the Nanoscope IIIa instrument operating in tapping mode with the oscillation frequency of around 300 kHz and the scan rate of about 1 Hz. The tip radius was typically of 4–7 nm. Roughness and section analysis of the obtained images were performed using the integrated image processing software.

3. Results and discussion

Typical absorption spectra of CdS and ZnS nanoparticles embedded in organic films of PAH and PSS are shown in Fig. 2(a) and (b). The absorption intensity increases monotonously with the increase in the number of layers, which reflects the consistency of electrostatic deposition. It has to be noted that the role of polyelectrolyte layers is crucial for successful deposition. The attempts of alternative deposition of layers of anion and cation modified nanoparticles without intermediate polyelectrolyte layers failed, because the first layer peeled off during the attempted deposition of the second layer. This was most likely due to a poor adhesion of the first layer of nanoparticles to the substrate.

As can be seen in the spectra presented in Fig. 2(a) and (b), the absorbance increases gradually starting from the absorption edge of about 405 nm for CdS, and 290 nm for ZnS. Both adsorption edges are blue shifted from the respective absorption bands of 512 nm and 335 nm for bulk CdS and ZnS materials. This is believed to be due to the effect of quantum confinement in the nanoparticles. The observation of the blue shift of optical absorption is a typical experimental confirmation of nanoparticles' presence [2,24,25]. Similar spectra were observed for CdS and ZnS nanoparticles capped with NH_2^+ groups. The inset of Fig. 2(a) and (b) shows the absorption spectra of CdS and ZnS colloid solutions which were almost the same as those for the electrostatically self-assembled films of CdS and ZnS.

The size of nanoparticles can be evaluated from the values of blue shift of the absorption bands [2,24]. Similar to the routine described earlier [25], in order to obtain the exact positions of absorption maxima, the Gaussian fitting of absorption spectra was performed and the spectra were re-plotted in energy coordinates (see Fig. 3(a) and (b)). The observed energy dispersion may reflect the combination of the size distribution of nanoparticles and the presence of higher index energy levels of size quantization [25]. Only the first maxima (in each spectrum) corresponding to the ground state levels were chosen for further analysis.

The radius of semiconductor clusters can be calculated using Efros equation for the electron energy spectrum in nanoparticles of direct band gap semiconductors, having parabolic

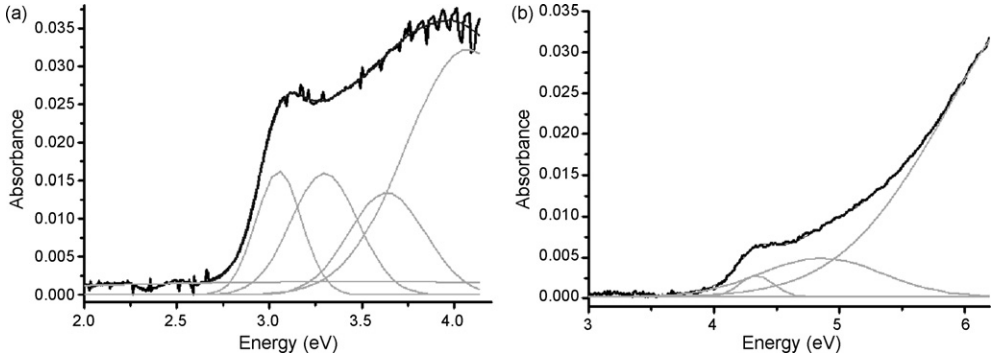

Fig. 3. Gaussian fitting of the spectra of the first layer of CdS–SO_3^- (a) and the first layer of ZnS–SO_3^- (b).

Table 1
The results of Gaussian fitting of the absorption spectra of CdS and ZnS nanoparticles

	E_1 (eV)	AE (eV)	Radius (nm)
CdS–SO_3^-	3.12 ± 0.0048	0.7	1.79 ± 0.01
CdS–NH_2^+	3.08 ± 0.0020	0.66	1.85 ± 0.01
ZnS–SO_3^-	4.34 ± 0.0121	0.66	1.80 ± 0.03
ZnS–NH_2^+	4.38 ± 0.0074	0.7	1.74 ± 0.02

$E(k)$ dispersion [24,25]:

$$E_{(n,1)} = E_g + \frac{\hbar^2}{2\mu R^2}\phi^2_{(n,1)} \quad (3)$$

Here E_g is the band gap for bulk semiconductors, μ the reduced effective mass of exciton, $(1/\mu) = (1/m_e^*) + (1/m_h^*)$, and $\phi_{(n,l)}$ are roots of Bessel functions (for the ground state $\phi_{(0,1)} = \pi$). Eq. (3) was based on the assumption of strong confinement in the particles smaller than Bohr exciton radius, respectively, 2.2 nm and 3 nm for ZnS and CdS [2], so that electrons and holes are quantized separately in the conduction and valence bands, respectively. The obtained values of CdS and ZnS nanoparticle size are summarized in Table 1.

The radius of nanoparticles of about 1.8 nm which are less than Bohr radius was obtained for both CdS and ZnS. Similar values were also obtained for respective nanoparticles in the colloid solution.

The ellipsometry measurements were carried out on thin polyelectrolite/nanoparticles films of deposited on pieces of silicon wafer. Typical ellipsometric spectra, of $\psi(\lambda)$ and $\Delta(\lambda)$ are shown in Fig. 4(a). These measurements confirmed the growth of polyelectrolyte/nanoparticles films on silicon. For example, the series of $\Delta(\lambda)$ spectra in Fig. 4(b) show their consecutive shift downwards after each layer being deposited, which corresponds to the increase in the film thickness.

Fitting the experimental ellipsometric spectra of Ψ and Δ using VWASE@ J.A. Woollam software allowed the extraction of the film thickness (d), and spectra of refractive index (n) and extinction coefficient (k) of all consecutively deposited layers. A multilayer model used for the ellipsometry fitting, shown in Tables 2 and 3, consists of Si substrate, SiO_2 layer representing a very thin (2–3 nm) film of native oxide, polyelectrolyte films of either PAH or PSS represented by Cauchy model, and the layers of either CdS or ZnS nanoparticles. The file names for models selected from the VWASE32® library are shown near respective layers in Tables 2 and 3. The default medium (air) was used everywhere. The parameters of all layers were obtained by fitting the spectra for consecutively deposited layers and fixing the previously obtained parameters for the layers below. For the transparent dielectric layers of polyelectrolytes (PAH or PSS) the value of $k = 0$ was fixed; and the variables were the thickness (d) and the parameter A in the Cauchy dispersion model [23]:

$$n = \frac{A+B}{\lambda^2} + \frac{C}{\lambda^4} \quad (4)$$

For the layers of CdS and ZnS nanoparticles the model files of respective bulk materials were used as initial guess; and all three parameters d, n, and k were varied during fitting.

Table 2
Ellipsometry data fitting of PAH/CdS–SO_3^- films

Model layer	d (nm)	n (at 633 nm)	k (at 633 nm)
Si (Si_gel.mat)		3.867	0.02
SiO_2 (SiO_2.mat)	5.99 ± 0.03	1.46	0
PAH (CAUCHY.mat)	1.94 ± 0.03	1.49	0
1st CdS (CDSO.mat)	4.94 ± 0.04	2.28	0.74
PAH (CAUCHY.mat)	2.12 ± 0.02	1.54	0
2nd CdS (CDSO.mat)	12.84 ± 0.02	1.82	0.74

Table 3
Ellipsometry data fitting of PAH/ZnS–SO_3^- films

Model layer	d (nm)	n (at 633 nm)	k (at 633 nm)
Si (Si_gel.mat)		3.867	0.02
SiO_2 (SiO_2.mat)	3.53 ± 0.05	1.46	0
PAH (CAUCHY.mat)	1.96 ± 0.06	1.49	0
1st ZnS (ZNS.mat)	5.24 ± 0.03	2.29	0.78
PAH (CAUCHY.mat)	2.24 ± 0.01	1.49	0
2nd ZnS (ZNS.mat)	5.53 ± 0.06	2.29	0.78

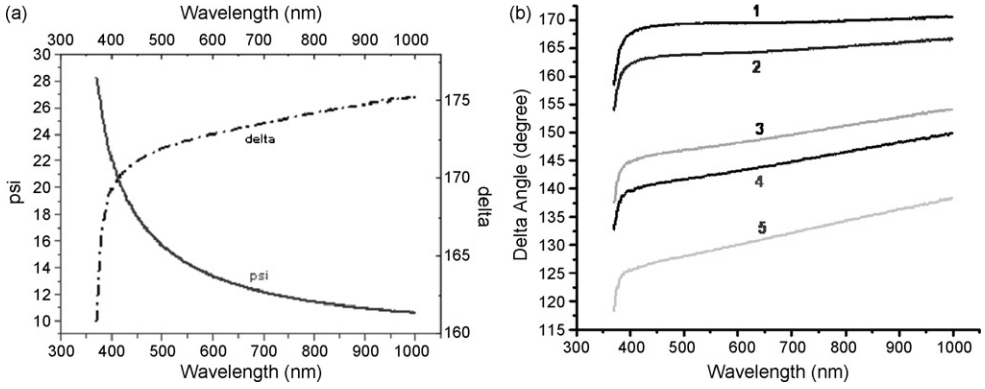

Fig. 4. (a) Typical $\psi(\lambda)$ and $\Delta(\lambda)$ ellipsometric spectra of silicon substrate. (b) Typical $\Delta(\lambda)$ ellipsometric spectra of silicon substrate (1), and consecutively deposited on top layers: 1st layer of PAH (2), 1st layer of ZnS nanoparticles (3), 2nd layer of PAH (4), and 2nd layer of ZnS nanoparticles (5).

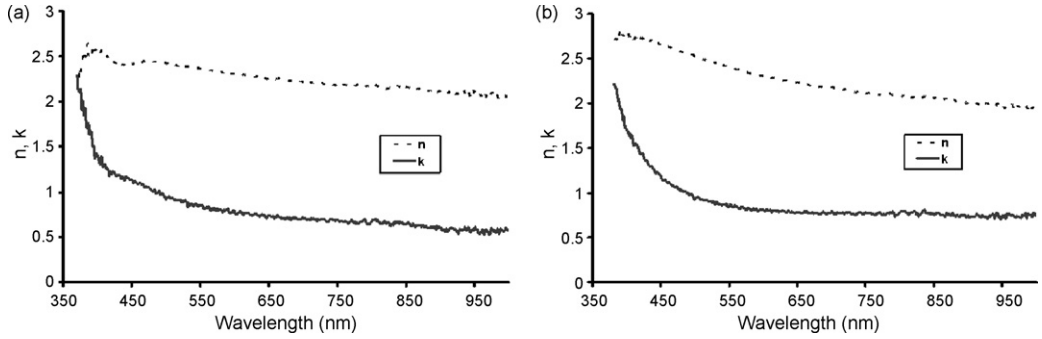

Fig. 5. The dispersion spectra of n and k obtained by ellipsometry data fitting for the first layer of CdS (a) and ZnS (b) nanoparticles.

The results of fitting are summarized in Tables 2 and 3. Although the whole spectra of n and k were obtained and shown in Fig. 5, only the values at 633 nm were presented. The obtained thicknesses of nanoparticle layers of around 5 nm for both CdS and ZnS correspond well to size of particles evaluated from UV–vis spectral data considering an additional thickness of the organic shell. The obtained larger thickness for the 2nd layer of CdS nanoparticles (see Table 2) is most likely due to the aggregation of nanoparticles.

The $n(\lambda)$ dispersion curves in Fig. 5(a) and (b) are typical to CdS and ZnS materials, respectively, though with slightly smaller values of n. For example, at the wavelength of 633 nm,

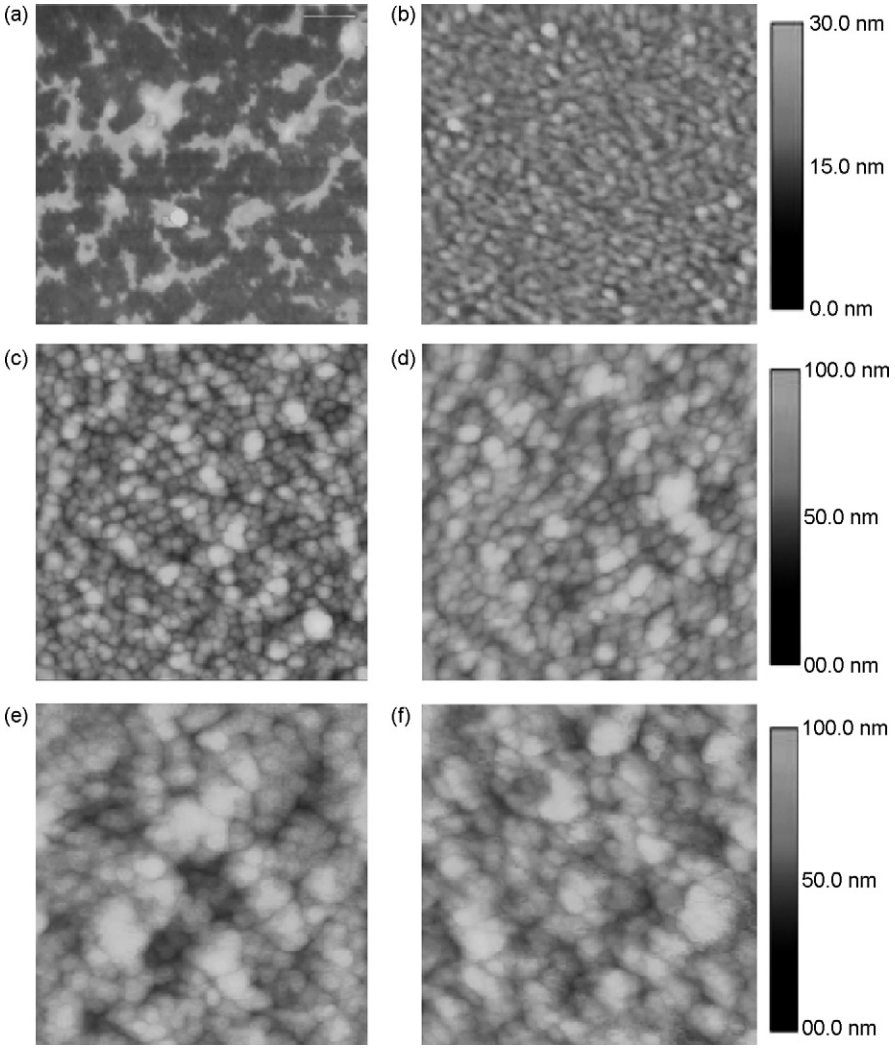

Fig. 6. Tapping mode AFM images (1 μm in size) of consecutively deposited layers of PAH (a), 1st PSS (b), 1st CdS–NH_2^+ (c), 2nd PSS (d), 2nd CdS–NH_2^+ (e), and 3rd PSS (f).

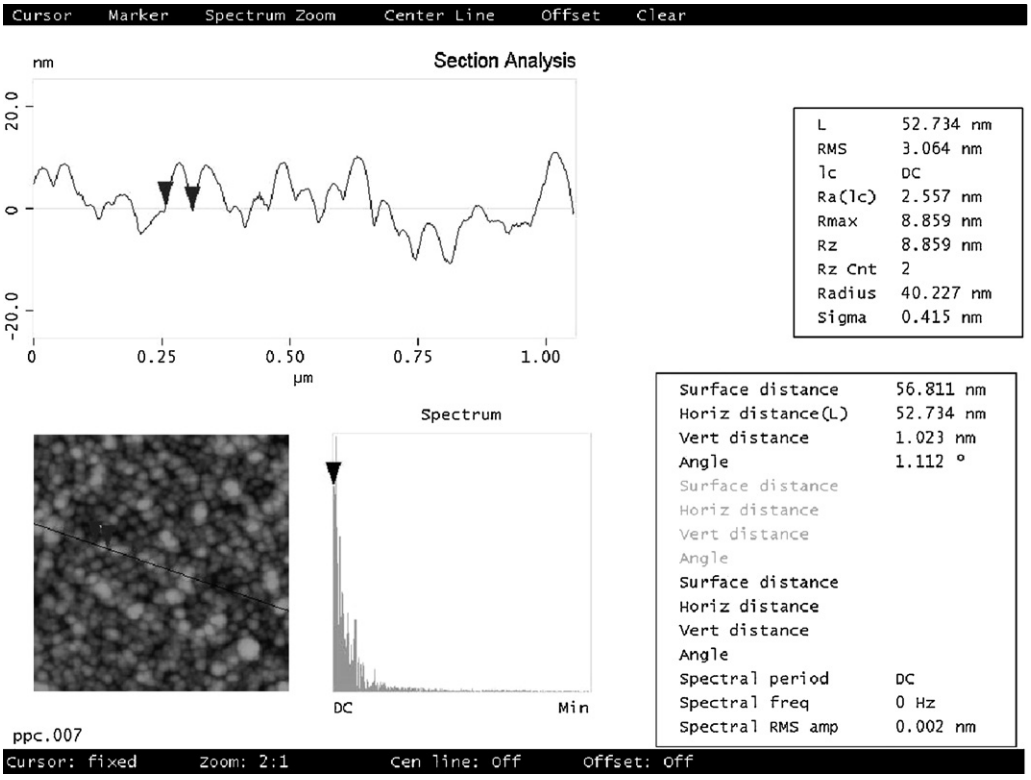

Fig. 7. Section analysis of tapping mode AFM images (1 μm in size) of the first CdS–NH_2^+ layer.

the obtained value of $n = 2.28$ is smaller than for 2.475 for bulk CdS, and the value of $n = 2.29$ is smaller than 2.364 for bulk ZnS. The $k(\lambda)$ dispersion curves in Fig. 5(a) and (b) resemble the respective absorption spectra of CdS films (Fig. 2(a)) and ZnS films (Fig. 2(b)) but values of k were deviated significantly from the respective values of bulk materials. For example, at the wavelength of 633 nm, the obtained value of $k = 0.74$ is significantly larger than 0.0186 for bulk CdS, as well as the value of $k = 0.78$ is much larger than 0.0077 for bulk ZnS. This may be attributed to the substantial increase in the oscillator strength due to the effect of quantum confinement in CdS and ZnS nanoclusters [24].

The obtained values of refractive index for polyelectrolyte layers of 1.49–1.54 are quite typical for PAH and PSS films, while the thickness of around 2 nm is slightly larger than reported previously [25], which may be caused by inhomogeneous coating.

In order to find out the structure and the size of the clusters, the AFM morphology study was carried out to the same types of films deposited on silicon. Typical tapping mode AFM images of consecutively deposited layers of polyelectrolytes and CdS colloid nanoparticles are shown in Figs. 6–8. It has to be noted that the images presented do not show the artifact features typically associated with either the blunt (damaged) tip or material accumulation on the tip and thus reproduce genuine surface profile of the samples [26]. Inclusions of different material, i.e. CdS (ZnS) clusters in the polymer matrix, can be seen on phase AFM images [26], which in our case are very similar to the presented height profiles. The roughness analysis was performed on every image presented, and the values of the mean roughness and RMS were presented in Tables 4 and 5 for the CdS and ZnS films, respectively.

The first PAH layer in Fig. 6(a) shows non-complete surface coverage. It is proved by the roughness analysis which gave the mean roughness of about 1.5 nm comparable to the thickness of PAH monolayer (see Table 4). The next layer of PSS (Fig. 6(b)) gave much more homogeneous coating (mean roughness of

Table 4
Summary of roughness parameters of polyelectrolyte/CdS films

Layer	Z range (nm)	Image RMS (nm)	Image mean (nm)
Silicon	2.0	0.2	0.1
1st PAH	30.4	2.2	1.5
1st PSS	6.9	0.7	0.5
1st CdS	32.2	3.9	3.0
2nd PSS	47.7	6.0	4.7
2nd CdS	61.7	8.9	6.9
3rd PSS	49.8	6.9	5.4

Table 5
Summary of roughness parameters of polyelectrolyte/ZnS films

Layer	Z range (nm)	Image RMS (nm)	Image mean (nm)
Silicon	2.0	0.2	0.1
1st PAH	30.4	2.2	1.5
1st ZnS	19.6	2.1	1.7
2nd PAH	19.8	2.2	1.7
2nd ZnS	27.9	3.7	2.9
3rd PAH	31.9	4.4	3.5

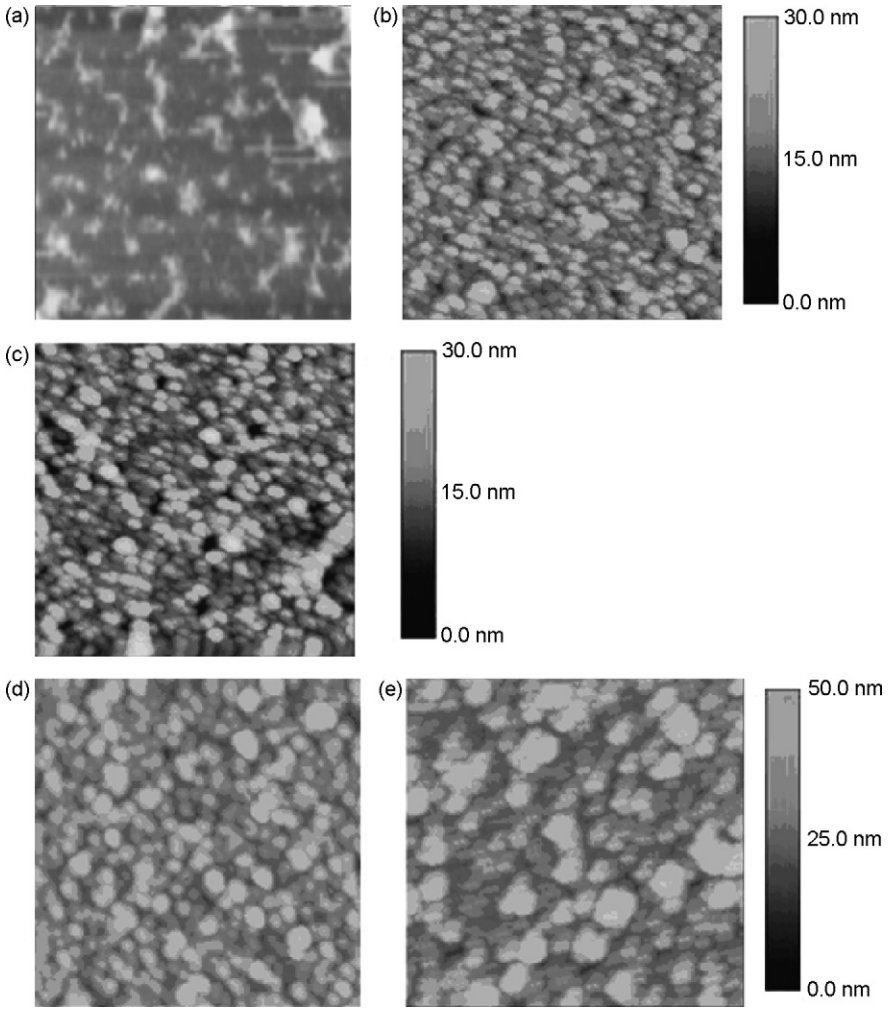

Fig. 8. Tapping mode AFM images (1 μm in size) of consecutively deposited layers of PAH (a), 1st ZnS–SO_3^- (b), 2nd PAH (c), 2nd ZnS–SO_3^- (d), and 3rd PAH (e).

0.5 nm) which is typical for PAH/PSS multilayered films. The deposition of CdS nanoparticles results in progressively rougher surface (see Table 4) due to the formation of large aggregates of CdS nanoparticles (Fig. 6(c–f)).

The size of the aggregates could be estimated directly from AFM height images in Fig. 6, however the section analysis and, particularly, particle analysis allows more precise quantification. For example, the section analysis of the first layer of CdS–SO_3^- in Fig. 7 reveals aggregates of nanoparticles of up to 50 nm in lateral size and 10 nm in height.

The particles analysis of the AFM image of the first CdS–NH_2^+ layer with the threshold height of 5 nm gave the value of around 28 nm as an average size of aggregates. The actual lateral size of the observed objects could be slightly smaller due to the finite tip radius of 4–7 nm [26].

A similar situation, i.e. the formation of aggregates and the roughness increase, were observed for PAH/ZnS–NH_2^+ films (see Fig. 8 and Table 5). The lateral size of ZnS aggregates in the range of 40–50 nm was estimated from the AFM images and confirmed by section and particle analysis.

It is suggested that the aggregation of either positively or negatively charged semiconductor nanoparticles, could only happen by intercalation of nanoparticles with the layers of polyanions (PSS) or polycations (PAH), respectively, as illustrated schematically in Fig. 9(a). This leads to the increase in the effective thickness and roughness of nanoparticle layers, often observed for the 2nd and following layers deposited.

The aggregation of nanoparticles could be reduced using diluted colloid solutions in the deposition process. Such experiments were performed; CdS nanoparticle films were deposited directly onto Si substrate from 100 and 500 times diluted colloid solutions, and the results were presented in Fig. 9(b) and (c), respectively.

Much smaller aggregates (groups) of nanoparticles are clearly visible on both images. In the case of 500 times diluted colloid solution the particle analysis of the AFM image in Fig. 9(c) reveals the groups of four particles with the average size (a) of about 18 nm. Considering the effective enlargement of lateral features of AFM images by a double tip radius [26], the actual size of CdS nanoparticles (a^*) can estimated as $a^* = a - 2r = 18 - 2 \times (4 \text{ to } 7) = 10$ to 4 nm, which is much closer to the expected particle size of 5 nm obtained with ellipsometry.

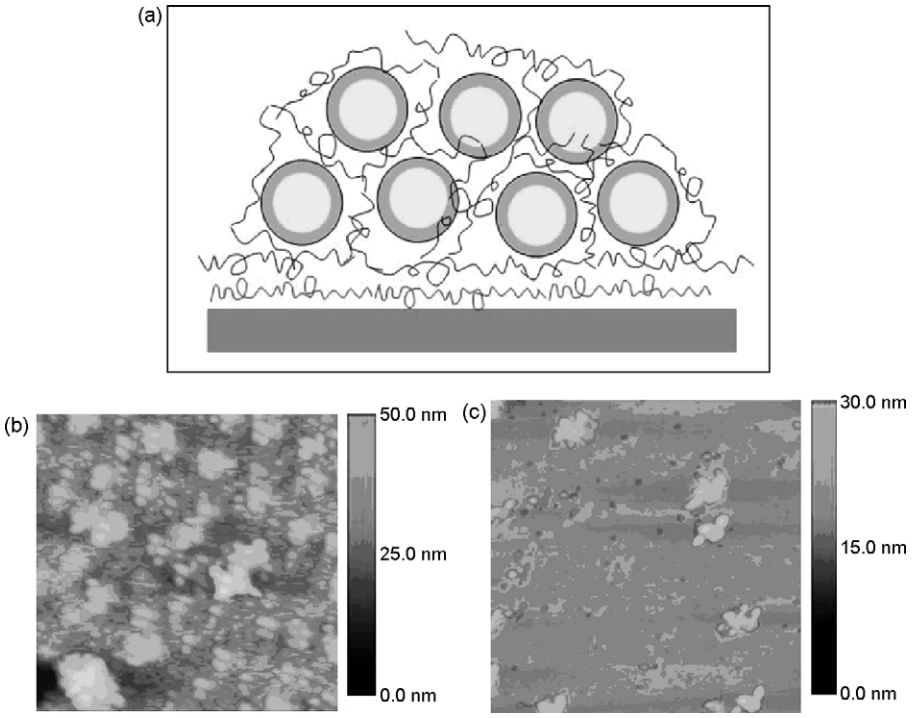

Fig. 9. The formation of aggregates of electrically charged nanoparticles by intercalation with polyelectrolytes (a). Tapping mode AFM images (1 μm in size) of CdS–NH_2^+ layers deposited from colloid solutions diluted in 100 times (b) and 500 times (c).

4. Conclusions

Electrically charged colloid nanoparticles were synthesized and successfully deposited onto quartz, glass, and silicon substrates using the method of electrostatic self-assembly. The particle core radius in the range of 1.8–1.9 nm for both CdS and ZnS nanoparticles was obtained from UV–vis absorption spectra. Ellipsometry gives slightly larger particle sizes (diameter) of about 5 nm due to the contribution of the organic shell. The dispersion spectra of n and k obtained from the ellipsometry data fitting are in line with the effect of quantum confinement observed in the absorption spectra. AFM shows large (40–50 nm) aggregates of electrically charged nanoparticles, which are most likely formed by the intercalation with oppositely charged polyelectrolytes. The size of aggregates can be reduced down to 12–20 nm by diluting the colloid solutions. Considering the AFM features' size enlargement due to a finite tip radius we may conclude that individual nanoparticles were observed with AFM.

References

[1] A.P. Alivisatos, J. Phys. Chem. 100 (1996) 13226–13239.
[2] A.D. Yoffe, Adv. Phys. 51 (2002) 799–890.
[3] M. Gao, C. Lesser, S. Richter, E. Kirstein, A.L. Möhwald, H. Rogach, Weller, J. Appl. Phys. 87 (2000) 2297–2302.
[4] M. Gao, B. Richter, S. Kirstein, Adv. Mater. 9 (1997) 802–805.
[5] M.E. Wozniak, A. Sen, Chem. Mater. 4 (1992) 753.
[6] Y. Wang, N. Herron, J. Phys. Chem. 92 (1988) 4988–4994.
[7] C. Petit, P. Lixon, M.P. Pileni, J. Phys. Chem. 94 (1990) 1598.
[8] C.B. Murray, D.B. Norris, M.G. Bawendi, J. Am. Chem. Soc. 115 (1993) 8706.
[9] N. Herron, Y Wang, H. Eckert, J. Am. Chem. Soc. 112 (1990) 1322–1326.
[10] T. Vossmeyer, L. Katsikas, M. Giersig, I.G. Popovic, K. Diesner, A. Chemseddine, A. Eychmuller, H. Weller, J. Phys. Chem. 98 (1994) 7665.
[11] Y. Nosaka, H. Shigeno, T. Ikeuchi, J. Phys. Chem. 99 (1996) 8317–8322.
[12] H.M. Chen, X.F. Huang, L. Xu, J. Xu, K.J. Chen, D. Feng, Superlattice Microstruct. 27 (2000) 1–5.
[13] A. Fojtik, H. Weller, U. Koch, A. Henglein, Ber. Bunsengesellschaft Phys. Chem. 88 (1984) 969–977.
[14] J.O. Winter, N. Gomez, S. Gatzert, C.E. Schmidt, B.A. Korgel, Colloid Surf. A: Physicochem. Eng. Aspects 254 (2004) 147–157.
[15] X. Peng, L. Manna, W. Yang, J. Wickham, E. Scher, A. Kadavanich, A.P. Alivisatos, Nature 404 (2000) 59–61.
[16] V.F. Puntes, K. Krishnan, A.P. Alivisatos, Top. Catal. 19 (2002) 145–148.
[17] Y. Lvov, G. Decher, Crystallogr. Rep. 39 (1994) 628–649.
[18] J.H. Fendler, Chem. Mater. 8 (1996) 1616–1624.
[19] M. Gao, B. Richter, S. Kirstein, H. Möhwald, J. Phys. Chem. B 102 (1998) 4096–4103.
[20] C. Lesser, M. Gao, S. Kirstein, Mater. Sci. Eng. C 8/9 (1999) 159–162.
[21] A.V. Nabok, A.K. Hassan, A.K. Ray, Mater. Sci. Eng. C 8/9 (1999) 505–508.
[22] R.M.A. Azzam, N.M. Bashara, Ellipsometry and Polarized Light, North-Holland, Amsterdam, 1977, pp. 153–169.
[23] Guide to Using WVASE32, J.A. Woollam Co. Inc., 2002.
[24] A.V. Nabok, T. Richardson, F. Davis, C.J.M. Stirling, Langmuir 13 (1997) 3198–3201.
[25] A.V. Nabok, T. Richardson, C. McCartney, N. Cowlam, F. Davis, C.J.M. Stirling, A.K. Ray, V. Gacem, A. Gibaud, Thin Solid Films 327–329 (1998) 510–514.
[26] Scanning Probe Microscopy Training Notebook, Version 3, Digital Instruments/Veeco Metrology Group Inc., 2000.